N-Glycosylation and Residue 96 Are Involved in the Functional Properties of UDP-Glucuronosyltransferase Enzymes[†,‡]

Olivier Barbier, Caroline Girard, Rock Breton, Alain Bélanger, and Dean W. Hum*

Oncology and Molecular Endocrinology Research Center, Laval University Medical Center (CHUL) and Laval University, Quebec, Quebec, G1V 4G2, Canada

Received April 5, 2000; Revised Manuscript Received June 7, 2000

ABSTRACT: The recent cloning of several human and monkey UDP-glucuronosyltransferase (UGT) 2B proteins has allowed the characterization of these steroid metabolic enzymes. However, relatively little is known about the structure−function relationship, and the potential post-translational modifications of these proteins. The mammalian UGT2B proteins contain at least one consensus asparagine-linked glycosylation site N*X*(S/T). Endoglycosidase H digestion of the human and monkey UGT2B proteins demonstrates that only UGT2B7, UGT2B15, UGT2B17, and UGT2B20 are glycosylated. Although UGT2B15 and UGT2B20 contain three and four potential glycosylation sites, respectively, site-directed mutagenesis revealed that both proteins are glycosylated at the same first site. In both proteins, abolishing glycosylation decreased glucuronidation activity; however, the K_m values and the substrate specificities were not affected. Despite the similarities between UGT2B15 and UGT2B20, UGT2B20 is largely more labile than UGT2B15. Treating HK293 cells stably expressing UGT2B20 with cycloheximide for 2 h decreased the enzyme activity by more than 50%, whereas the activity of UGT2B15 remained unchanged after 24 h. The UGT2B20 protein is unique in having an isoleucine at position 96 instead of an arginine as found in all the other UGT2B enzymes. Changing the isoleucine in UGT2B20 to an arginine stabilized enzyme activity, while the reciprocal mutation in UGT2B15 R96I produced a more labile enzyme. Secondary structure predictions of UGT2B proteins revealed a putative α-helix in this region in all the human and monkey proteins. This α-helix is shortest in UGT2B20; however, the helix is lengthened in UGT2B20 I96R. Thus, it is apparent that the length of the putative α-helix between residues 84 and 100 is a determining factor in the stability of UGT2B enzyme activity. This study reveals the extent and importance of protein glycosylation on UGT2B enzyme activity and that the effect of residue 96 on UGT2B enzyme stability is correlated to the length of a putative α-helix.

Glucuronidation is an important metabolic pathway for numerous endogenous and exogenous compounds, including drugs, phenolic compounds, bile acids, bilirubine, and steroid hormones (*1*−*3*). In this reaction, the glucuronosyl moiety of UDP-glucuronic acid (UDPGA)[1] is transferred to a hydrophobic aglycone, which becomes more hydrosoluble, generally less active, and more easily excreted from the body via the bile or urine (*1*). This process is catalyzed by UDP-glucuronosyltransferase (UGT) enzymes, which are membrane-associated proteins of the endoplamic reticulum (ER). To date, more than 61 different UGT cDNAs have been cloned in several mammalian species, including rats, rabbits, monkeys, and humans. On the basis of the homology of primary structures, the UGT proteins have been categorized into two major families, UGT1 and UGT2, with the UGT2 family further divided into two groups, UGT2A and UGT2B (*2*). Enzymes of the UGT2B subfamily catalyze the glucuronidation of several endogenous compounds, including bile acids, steroid hormones, fatty acids, and carboxylic acids (*2*). The characterization of human UGT2B enzymes demonstrates an overlap of substrate specificities between the different proteins. However, each enzyme is active on specific classes of steroids, which are glucuronidated at their hydroxyl groups.

In eukaryotes, many metabolic enzymes associated with the ER undergo post-translational modifications such as removal of the signal sequence and asparagine-linked glycosylation (N-glycosylation), following translocation into the lumen (*4*). Post-translational N-glycosylation is known to regulate protein functions. For example, the catalytic activity of lipase (*5*) and β-glucuronidase (*6*) is decreased, and the prolactin receptor has a lower affinity (*7*) following deglycosylation. The human UGT1A6, UGT2B15, and monkey UGT2B20 proteins have been shown to be glycosylated, while monkey UGT2B23 is not (*8*−*10*). However, the role

[†] This work was supported by the Medical Research Council of Canada (D.W.H. and A.B.), the Fonds de la Recherche en Santé du Québec (D.W.H.), and Endorecherche.

[‡] Genbank accession numbers for the human enzymes: UGT2B4, Y00317; UGT2B7, J05428; UGT2B15, U08854; UGT2B17, U59209. Genbank accession numbers for the monkey enzymes: UGT2B9, U91582; UGT2B18, AF016310; UGT2B19, AF112112; UGT2B20, AF072223; UGT2B23, AF112113.

* To whom correspondence should be addressed: Oncology and Molecular Endocrinology Research Center, 2705 Boulevard Laurier, Quebec, Quebec G1V 4G2, Canada. Telephone: (418) 654-2296. Fax: (418) 654-2279. E-mail: dean.hum@crchul.ulaval.ca.

[1] Abbreviations: UGT, uridine-diphosphoglucuronosyltransferase; UDPGA, UDP-glucuronic acid; 3α-diol, 5α-androstane-3α,17β-diol; DHT, dihydrotestosterone.

10.1021/bi000779p CCC: $19.00
Published on Web 08/30/2000

of glycosylation of these proteins remains unknown. Tunicamycin treatment of COS cells stably expressing rat UGT2B1 and UGT2B2 produced faster migrating deglycosylated proteins upon SDS−PAGE. These deglycosylated proteins retained the same substrate specificity, but had decreased glucuronidation velocities (*11*).

Interestingly, the two glycosyltransferase activities, glucuronidation and N-glycosylation, have been proposed to be closely related and mutually regulated in terms of their expression. Lidholt et al. (*12*) characterized a Chinese hamster ovary cell line (pgsD-677), which expressed reduced *N*-acetylglucosaminyltransferase activity (GlcNAc), required to initiate the synthesis of N-linked carbohydrate formation, and the cells also had reduced UGT activity. Thus, it was suggested this may be due to mutation of a transcription factor required for the regulation of both genes. Moreover, expression of UGT, GlcNAc, and UDP-*N*-acetylglucosamine: dolichylphosphate *N*-acetylglucosamine-1-phosphate transferase (GPT), an enzyme which is involved in the dodichol pathway of protein N-glycosylation, is upregulated by retinoic acid (*13*, *14*).

To date, the tertiary structure of UGT enzymes has not been derived due to the inherent difficulties in obtaining crystals of membrane-associated proteins. The purification of UGT enzymes requiring delipidation often results in inactivation, and reconstitution with lipids is generally needed to restore full function (*15*, *16*). Moreover, in some cases, purified and expressed UGT isoforms have demonstrated different substrate profiles (*16*). To investigate the structure−function relationship of UGT2B enzymes, site-directed mutagenesis and the formation of chimeric proteins have identified putative substrate binding domains. Via exchange of the amino and carboxyl regions between different UGT2B enzymes, the aglycone specificity domain is proposed to be in the amino-terminal half of the protein, whereas the conserved carboxyl-terminal domain binds the common cofactor UDPGA (*17*, *18*). The conserved region between residues 350 and 400 has been postulated to be an important component of the UDPGA-binding site (*2*). Using site-directed mutagenesis, it has been shown that residues R52 and H54 are important for UGT function, probably by maintaining protein structural integrity (*19*). Progressive truncation of the protein from the carboxyl terminus was shown to reduce enzyme activity (*20*). On the other hand, Li et al. (*21*) demonstrated that the carboxyl-terminal region of UGT proteins may play a critical role in catalytic activity, where the region between amino acids 434 and 531 may be involved in conformational stability. A recent study demonstrated that residue 121 in the amino-terminal region is important for catalytic activity of UGT2B15 and for the 3α-hydroxysteroid stereospecificity of UGT2B17 (*22*).

The monkey UGT2B20 enzyme was recently cloned, characterized, and shown to conjugate androgen metabolites (*9*). This protein is highly homologous to the human UGT2B15 enzyme (*23*), which contains only 41 amino acid differences. The two enzymes have similar substrate specificities and kinetic characteristics for 3α-diol and dihydrotestosterone (DHT) glucuronidation. However, two important differences exist between the two enzymes. First, UGT2B20 contains four potential N-linked glycosylation sites, while UGT2B15 has only three sites; second, UGT2B15 enzyme activity is largely more stable than that of UGT2B20. When HK293 cells expressing the two proteins are incubated with cycloheximide, an inhibitor of protein synthesis, the catalytic activity of UGT2B20 is decreased by at least 50%, while the same treatment has no effect on UGT2B15 (*9*, *24*). In this study, the extent of UGT2B protein glycosylation was assessed, and the site of glycosylation on UGT2B20 and UGT2B15 was determined. For both enzymes, abolishing the glycosylation site had an effect on enzyme activity. Exchanging specific amino acids in a variable region between UGT2B20 and UGT2B15 revealed the importance of residue 96, which influences the stability of enzyme activity via an effect on a putative α-helix predicted in all mammalian UGT2B proteins.

EXPERIMENTAL PROCEDURES

Materials. The QuikChange site-directed mutagenesis kit, restriction enzymes, and other molecular biology reagents were from Stratagene (La Jolla, CA), Pharmacia LKB Biotechnology Inc. (Milwaukee, WI), Gibco BRL, and Boehringer Mannheim (Indianapolis, IN). Human embryonic kidney 293 cells (HK293) were obtained from the American Type Culture Collection (Rockville, MD). Lipofectin and Geneticin (G418) were obtained from Gibco BRL. Blasticidin was from Invitrogen Corp. (Carlsbad, CA). Protein assay reagents were obtained from Bio-Rad (Richmond, CA). Cycloheximide and all aglycons were obtained from Sigma Chemical Co. (St. Louis, MO) and ICN Pharmaceutical Inc. Radioinert steroids were purchased from Steraloids Inc. (Wilton, NH). Radiolabeled [9,11-^{3}H]androstane-3α,17β-diol (56 Ci/mmol), [1,2-^{3}H]dihydrotestosterone (47 Ci/mmol), and [1,2,6,7-^{3}H]testosterone (90 Ci/mmol) were obtained from NEN Dupont (Boston, MA). The UGT2B cDNAs and stable cell lines were obtained as previously described (*9*, *10*, *25*−*31*).

Site-Directed Mutagenesis of UGT2B15, UGT2B17, and UGT2B20. The mutations were performed using the QuikChange site-directed mutagenesis system (Stratagene). Using wild-type pcDNA6-UGT2B15, pBK-CMV-UGT2B17, and pBK-CMV-UGT2B20 cDNAs (50 ng), the substitution of amino acids was carried out following polymerase chain reaction (PCR) amplification. The experimental conditions were as follows: 10 mM KCl, 10 mM $(NH_4)_2SO_4$, 20 mM Tris-HCl (pH 8.8), 2 mM $MgSO_4$, 0.1% Triton X-100, 0.1 mg/mL BSA, 10 mM dNTP, and 2.5 units of Pfu DNA polymerase in a total volume of 50 μL. The reactions were carried out using 125 ng of specific primers containing the mutation (Table 1). PCRs were performed for 21 cycles (30 s at 94 °C, 1 min at 55 °C, and 6 min at 68 °C). The PCR products were treated with 10 units of *Dpn*I endonuclease, and 1 μL was transformed in 50 μL of *Escherichia coli* (Epicurian Coli XL1-Blue) supercompetent cells. All the UGT2B15, UGT2B17, and UGT2B20 mutated plasmids were sequenced in both directions to confirm the presence of the incorporated mutation. The sites of the mutation performed on the isoenzymes are indicated in Figure 1.

With regard to UGT2B20 stability analysis, all amino acid substitutions were performed for the amino acid at the corresponding position of the low labile UGT2B15 protein (UGT2B20 L93I, I96R, T98I, and S100G); using the UGT2B20 I96R cDNA, a double mutation was produced as UGT2B20 I96R/T98I (Table 1). Inverse mutations in

Table 1: Primers Used for Site-Directed Mutagenesis of UGT2B15, UGT2B17, and UGT2B20[a]

Mutants	Oligonucleotides
UGT2B20 L93I	-CT-CTT-ATG-AAA-**A**T**T**-CTA-GAT-ATT-TGG-AC-
UGT2B20 I96R	-G-AAA-CTG-CTA-GAT-A**G**A-TGG-ACA-TAT-AGT-
UGT2B20 T98I	-G-CTA-GAT-ATT-TGG-A**T**A-TAT-AGT-ATT-TC-
UGT2B20 S100G	-ATT-TGG-ACA-TAT-**G**GT-ATT-TCA-AAC-AGT-
UGT2B20 I96R T98I	-CTG-CTA-GAT-A**GA**-TGG-A**T**A-TAT-AGT-A
UGT2B15 R96I	-TT-CTC-GAT-A**TT**-TGG-ATA-TAT-GGT-
UGT2B15 I98T	-CTC-GAT-AGA-TGG-A**C**A-TAT-GGT-GTT-TCA-
UGT2B15 R96I I98T	-CTC-GAT-A**TT**-TGG-A**C**A-TAT-GGT-GTT-TCA-
UGT2B17 T98I	-TTC-GAT-AGA-TGG-A**T**A-TAT-AGT-ATT-TCA-
B20Site1 (N65D)	-GCT-TCT-ACT-GTC-**G**AT-GAC-AGT-AAA-TCA-TCT-G-
B20Site1′ (N103K)	-ACA-TAT-AGT-ATT-TCA-AA**A**-AGT-ACA-TTT-TTG-
B20Site2 (S316E)	-G-TCG-ATG-ATC-AGT-AAC-ATG-**GA**A-GAA-GAA-AG-
B20Site3 (N483D)	-GTC-GCA-GCT-CAC-**G**AC-CTC-ACC-TGG-ATC-CAG-
B15Site1 (N65D)	-G-GCT-TCT-ACT-CTT-GTC-**G**AT-GCC-AGT-AAA-TCA-
B15Site2 (S316E)	-G-TCG-ATG-ATC-AGT-AAC-ATG-**GA**A-GAA-GAA-AG-
B15Site3 (N483D)	-GTC-GCA-GCT-CAC-**G**AC-CTC-ACC-TGG-ATC-CAG-

[a] Nucleotides producing amino acid changes are in bold and underlined.

UGT2B15 were produced at positions 96 and 98 (UGT2B15 R96I and I98T), and the corresponding double mutant (UGT2B15 R96I/I98T) was obtained using these cDNAs as the DNA template. In the UGT2B17 amino acid sequence, only Thr98 was changed for the Ile, as found in UGT2B15 (Table 1 and Figure 1).

For studying the role of glycosylation, an amino acid residue was changed at all N-linked glycosylation potential sites of UGT2B15 and UGT2B20 as indicated in the Table 1. Potential glycosylation sites were named in order of their location on the UGT2B protein (site 1, site 2, and site 3), and the additionnal site of UGT2B20 was named site 1′ (Figure 1). For mutation of this site, Asn103 of UGT2B20 was replaced with the Lys of UGT2B15 (B20Site1′); in UGT2B15 and UGT2B20 sequences, N65 (B15Site1 and B20Site1) and N483 (B15Site3 and B20Site3) were replaced with an aspartic acid residue as found in all other human and monkey UGT2B proteins, and Ser318 (B15Site2 and B20Site2) was changed for a Glu as found in monkey UGT2B9. To ensure the integrity of the cDNAs produced and to assess the presence of the directed mutation, cDNAs were sequenced in both directions by dideoxy sequencing using oligonucleotides.

In Vitro Transcription and Translation of Wild-Type and Mutant cDNAs. The entire cDNAs in the pBK-CMV or pcDNA6 expression vector were transcribed and translated using T3 or T7 RNA polymerase in the transcription/translation-coupled rabbit reticulocyte lysate system from Promega (Madison, WI) in the presence of [^{35}S]methionine. The protein products were separated on a 10% SDS/polyacrylamide gel and exposed on Hyperfilm-MP (Kodak Corp., Rochester, NY) for 1 h.

Stable Expression of Wild-Type and Mutant UGT2B15, UGT2B17, and UGT2B20 Proteins. HK293 cells were grown in Dulbecco's modified Eagle's medium containing 4.5 g/L glucose, 10 mM HEPES, 110 μg/mL sodium pyruvate, 100 IU of penicillin/mL, 100 μg/mL streptomycin, and 10% fetal bovine serum (FBS) in a humidified incubator, with an atmosphere of 5% CO_2, at 37 °C. The entire cDNA (5 μg) containing wild-type or mutated human and monkey UGT2B was transfected into HK293 cells using Lipofectin. Stable transfectants were selected in medium containing 1 mg/mL G418 or 5 μg/mL Blasticidine as previously reported (*27*).

Microsomal Protein Isolation. Transfected and untransfected HK293 cells (8×10^6) were frozen and thawed three times in liquid nitrogen and then homogenized in 5 mL of homogenization buffer [0.1 M K_2HPO_4, 0.1 M KH_2PO_4 (pH 7.4), 20% glycerol, 1 mM EDTA, 1 mM dithiothreitol, 2.5 μg/mL pepstatin, and 0.5 μg/mL leupeptin] using a Potter-Glas-col (Terre Haute, IN) homogenizer with a Teflon pestle at 4 °C, and centrifuged at 12000*g* and 4 °C for 20 min. The supernatant was centrifuged at 105000*g* for 1 h at 4 °C. The microsome pellets were resuspended in 0.5 mL of homogenization buffer.

Endoglycosidase H Digestion and Immunoblot Analysis. Microsomal proteins from HK293 cells stably expressing human and monkey UGT2B (25 μg) were incubated with 20 munits of endoglycosidase H in the presence of 50 mM sodium acetate (pH 5.5) and 0.1% SDS in a final volume of 20 μL for 16 h at 37 °C (*10*). Proteins were separated on a 10% SDS−polyacrylamide gel, transferred onto nitrocellulose membrane, and probed with the EL-93 anti-UGT2B antisera (1:3000 dilution) as reported previously (*26*). An anti-rabbit IgG horse antibody conjugated with peroxidase (Amersham) was used as the second antibody, and the resulting immunocomplexes were visualized using a chemiluminescence kit (ECL) (Renaissance) and exposed on hyperfilm (Kodak Corp.) for 20 s or 1 or 5 min depending on the level of the protein that is expressed.

Immunoblot Analysis of Wild-Type and Mutant Proteins. Microsomal proteins (20 μg) of untransfected HK293 cells and HK293 cells stably expressing wild-type and mutated UGT2B15, UGT2B17, and UGT2B20 were separated by size on a 10% SDS−polyacrylamide gel, transferred onto a nitrocellulose membrane, and probed with the EL-93 anti-UGT2B antisera (1:3000 dilution) or with anticalnexin CT antibody (StressGen Biotechnologies Corp., Victoria, Canada, 1:1000 dilution). An anti-rabbit IgG antibody conjugated with peroxidase (Amersham) was used as the second antibody, and the resulting immunocomplexes were visualized using a chemiluminescence kit (ECL) (Renaissance) and exposed on hyperfilm for 1 min (Kodak Corp.) and quantified by BioImage Visage 110s from Genomic Solution Inc. (Ann Arbor, MI). To ensure that equal amounts of protein from the control (untransfected) and stably transfected cells were loaded in each lane of the Western blot analysis, the same quantity of protein, as with the anti-UGT2B antibody, was probed with an anticalnexin antibody. To further analyze the relative level of protein expression in stably expressing cells, UGT2B and calnexin proteins were quantified and compared as follows. Staining with the anti-UGT2B antibody was normalized using the corresponding signal obtained with anticalnexin antibody, and the ratio for each mutant was compared to those of the related wild-type protein.

Glucuronidation Assay Using Intact Cells. Intact HK293 cells were incubated with radiolabeled steroid substrates as previously described (*27*). Cells were incubated for 6 h at 37 °C with 5, 10, and 20 μM radioinert 3α-diol, DHT, and testosterone, repectively, and the corresponding radiolabeled substrate (20 nM). The medium was removed and analyzed for glucuronide conjugates by organic extraction and scintillation counting as previously described (*32*). The data that were obtained were normalized by protein contents.

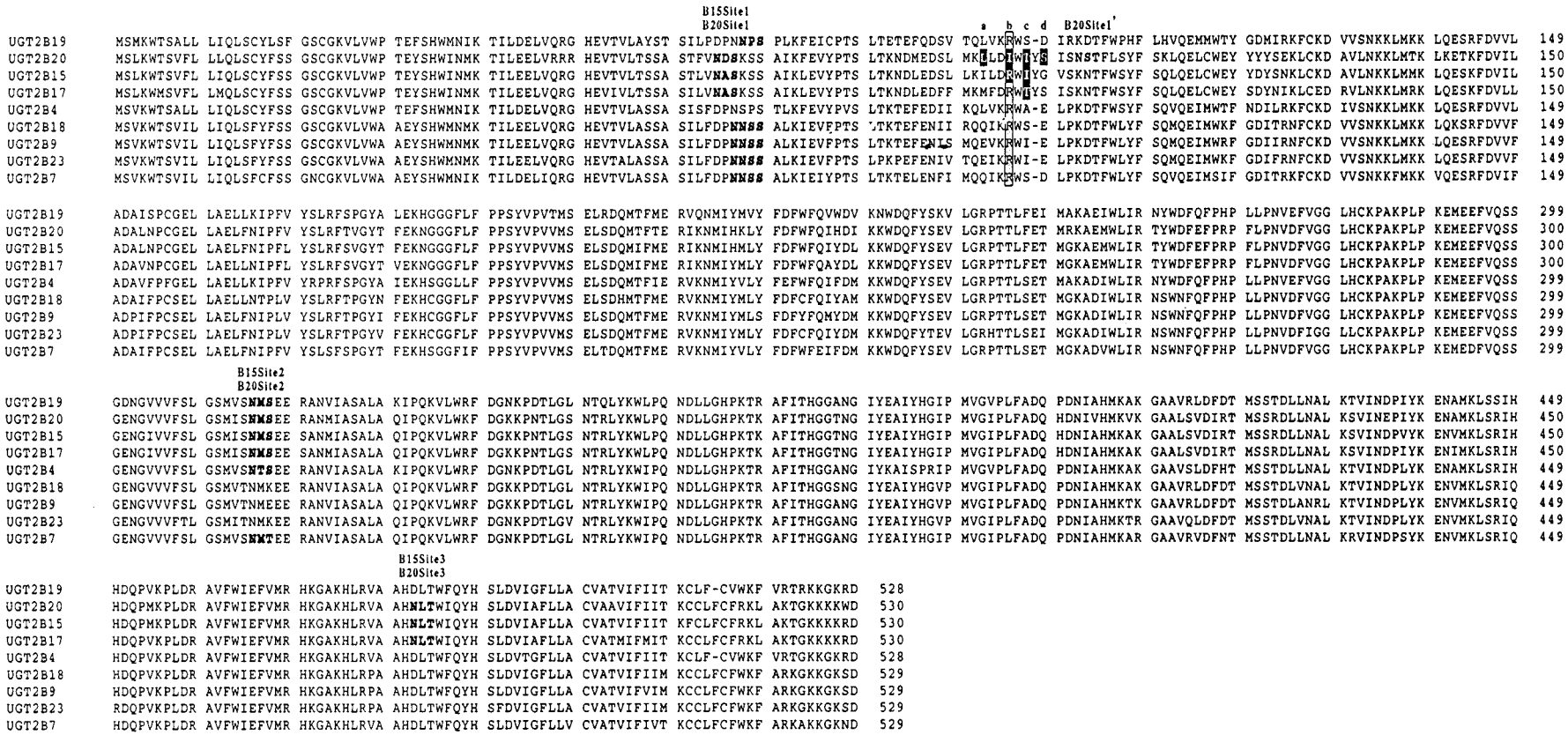

Protein	Number of potential glycosylation sites	Positions of potential N-linked glycosylation sites			
UGT2B4	1	315-NTS.			
UGT2B7	3	67-NNS;	68-NSS;	315-NMT.	
UGT2B15	3	65-NAS;	316-NMS;	483-NLT.	
UGT2B17	3	65-NAS;	316-NMS;	483-NLT.	
UGT2B9	2	67-NNS;	68-NSS		
UGT2B18	2	67-NNS;	68-NSS		
UGT2B19	2	68-NPS;	315-NMS.		
UGT2B20	4	65-NDS;	103-NST;	316-NMS;	483-NLT.
UGT2B23	2	67-NNS;	68-NSS.		

FIGURE 1: Comparison of N-linked glycosylation sites in the primary structure of human and monkey UGT2B enzymes. The potential N-linked glycosylation sites are in bold, and the residues in boxes were changed by site-directed mutagenesis. The mutations as indicated at the top of the amino acids sequences are (a) UGT2B20 L93I, (b) UGT2B20 I96R and UGT2B15 R96I, (c) UGT2B20 T98I, UGT2B15 I98T, and UGT2B17 T98I, (d) UGT2B20 S100G, (B15Site1) UGT2B15 N65D, (B20Site1) UGT2B20 N65D, (B20Site1′) UGT2B20 N103K, (B15Site2) UGT2B15 S316E, (B20Site2) UGT2B20 S316E, (B15Site3) UGT2B15 N483D, and (B20Site3) UGT2B20 N483D. The clear box indicates position 96 in all the human and monkey UGT2B proteins.

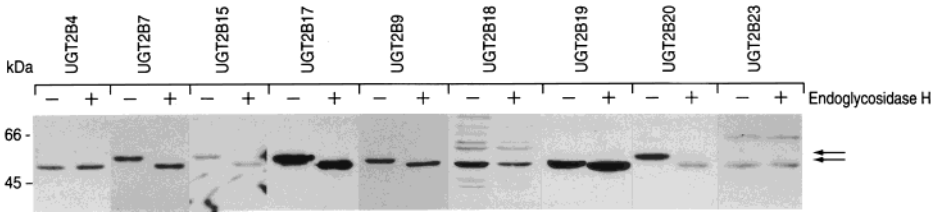

FIGURE 2: Western blot analysis of human and monkey UGT2B protein glycosylation by digestion with endoglycosidase H. Microsomal proteins isolated from transfected HK293 cells expressing human and monkey UGT2B proteins (25 μg) were digested by endoglycosidase H. Proteins were separated on a 10% SDS−polyacrylamide gel and transferred onto nitrocellulose, and the membrane was probed with the anti-UGT2B17 polyclonal antibody (EL-93). The top arrow on the right indicates the immunoreactive protein(s) seen in HK293 cells expressing UGT2B7, UGT2B15, UGT2B17, and UGT2B20. The bottom arrow indicates the faster migrating immunoreactive protein seen in these microsomes following endoglycosidase H treatment. The migration of other UGT2Bs is not altered following endoglycosidase H treatment, and it comigrates with the deglycosylated proteins seen with UGT2B7, UGT2B15, UGT2B17, and UGT2B20 microsomes.

In Vivo Protein Stability Analysis. Wild-type and mutant human and monkey UGT2B-HK293-transfected cells were plated at a density of 2×10^5 cells per well in a 24-well plastic plate and treated with 20 μg/mL cycloheximide for 2 h. After treatment, cells were incubated in the presence of medium containing 20 μg/mL cycloheximide, radioinert 3α-diol (10 μM), and 20 nM [^{3}H]-3α-diol for 6 h. To determine the protein half-life, transfected cells were reassayed under the same conditions, with cycloheximide pretreatment for 1, 2, 4, 6, 8, 10, 12, and 24 h (*9*). The data were normalized by protein measurement using the Bradford method.

K_m Determination in Intact HK293 Cells. K_m determinations were performed by incubating intact stably transfected HK293 cells with radiolabeled steroid substrates as described above. Cells were incubated for 6 h at 37 °C with 0.5, 1, 2.5, 5, 10, and 20 μM radioinert 3α-diol or DHT and the corresponding radiolabeled substrate (20 nM).

Protein Secondary Structure Prediction. The effect of mutations on the predicted structure of UGT2B20, UGT2B20 I96R, UGT2B15, and UGT2B15 R96I was predicted using six different algorithms: J. Levin (*33*), B. Rost and C. Sander (*34*), D. Frishman and P. Argos (*35*), D. G. Kneller et al. (*36*), T. Yi and E. Lander (*37*), and J. U. Bowie et al. (*38*). To further understand the role of these mutations, all human and monkey UGT2B proteins and all mutant proteins were reanalyzed using the methods of J. Levin and D. Frishman, and P. Argos.

RESULTS

Potential N-Glycosylation Sites of Active UGT2B Enzymes. To assess the importance of glycosylation in UGT2B enzymes, primary structure comparison between the active human (UGT2B4, UGT2B7, UGT2B15, and UGT2B17) and monkey (UGT2B9, UGT2B18, UGT2B19, UGT2B20, and UGT2B23) proteins shows differences in the number of potential asparagine-linked glycosylation sites with the sequence N*X*(S/T) (Figure 1). The UGT2B4 protein contains only one site. UGT2B9, UGT2B18, UGT2B19, and UGT2B23 have two sites. UGT2B7, UGT2B15, and UGT2B17 contain three sites. UGT2B20 is unique in having four potential sites. Except for UGT2B4, all of the enzymes have at least one site between amino acids 65 and 70, whereas UGT2B7, UGT2B9, UGT2B18, and UGT2B23 have two overlapping sites in this region. The locations of glycosylation sites are conserved between UGT2B15, UGT2B17, and UGT2B20; however, UGT2B20 contains an additional site found between the first and the second (Figure 1).

To determine if the UGT2B proteins are indeed glycosylated, microsomal proteins isolated from HK293 cells stably expressing human and monkey UGT2B cDNAs were digested by endoglycosidase H and separated on SDS−PAGE, and proteins were detected by Western blotting using the EL-93 anti-UGT2B antisera as a probe (Figure 2). The faster migration of UGT2B7, UGT2B15, UGT2B17, and UGT2B20 following endoglycosidase H digestion is indicative of these proteins being deglycosylated. However, the migration of the other UGT2B proteins with an apparent molecular mass of approximately 51 kDa remained the same (Figure 2). These results agree with previous data indicating that UGT2B23 was not glycosylated, and that tunicamycin treatment of HK293 cells expressing UGT2B15 and UGT2B20 yielded faster migrating deglycosylated proteins (*9*, *10*).

Sites of Human and Monkey UGT2B Protein N-Glycosylation. To determine the site(s) of N-glycosylation in UGT2B15 and UGT2B20, and to assess the importance of glycosylation on enzymatic properties, each potential site was mutated by site-directed mutagenesis. To confirm that the mutated UGT2B cDNAs encode proteins as predicted by the open reading frames, in vitro transcription and translation reactions produced 51 kDa proteins as expected (Figure 3A).

To further analyze the wild-type and mutant UGT2B proteins, cDNAs were stably transfected into HK293 cells, and the derived cell lines were demonstrated to express UGT2B proteins as determined by Western blot analysis (Figure 3B). Expression of the variant B15Site1 cDNA, which was mutated at the first potential glycosylation site from the amino terminus, produced a protein with an apparent molecular mass that was lower than that of the wild type. However, the B15Site2 and B15Site3 proteins, which were mutated at the second and third potential glycosylation sites, respectively, had the same apparent molecular mass as wild-type UGT2B15 (Figure 3B). Thus, these results are indicative of UGT2B15 being glycosylated at site 1 only.

Expression of the mutant B20Site1 cDNA produced a protein with an apparent molecular mass that was lower than that of the wild type, whereas there was little apparent difference in the relative mobilities of B20Site1′, B20Site2, B20Site3, and UGT2B20 proteins on SDS−PAGE (Figure 3B). Thus, as found for UGT2B15, it is apparent that UGT2B20 is also glycosylated at the first site located in the amino-terminal portion of the protein.

Effect of N-Glycosylation on Enzyme Activity, Stability, and Kinetic Properties. To analyze the role of glycosylation in UGT2B15 and UGT2B20, the enzyme activities of wild-

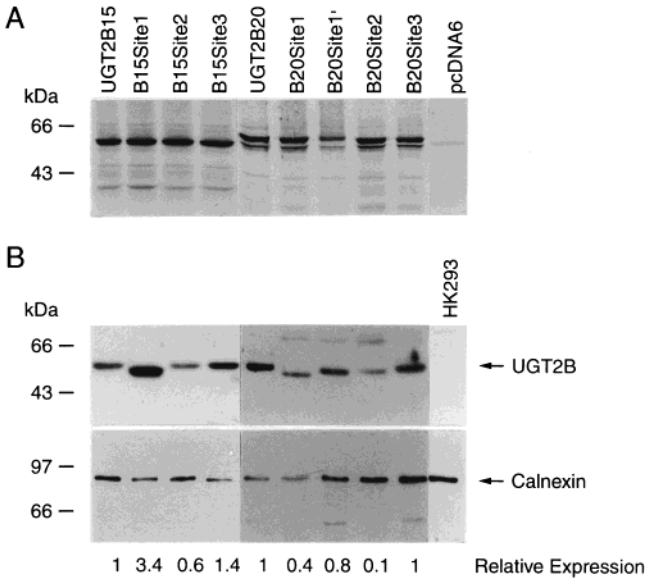

FIGURE 3: (A) In vitro transcription/translation of wild-type and mutant UGT2B cDNA clones and (B) immunoblot analysis of HK293 cells stably expressing N-glycosylation mutant UGT2B proteins. (A) The products of an in vitro transcription/translation reaction of wild-type and mutant UGT2B cDNAs and the pcDNA6 vector were separated by 10% SDS−PAGE. (B) Microsomal proteins (20 μg) from untransfected HK293 cells and HK293 cells stably expressing wild-type and glycosylation mutants of UGT2B15 and UGT2B20 were separated on a 10% SDS−polyacrylamide gel, transferred onto a nitrocellulose membrane, and probed with (upper panel) the EL-93 anti-UGT2B antisera (1:3000 dilution) or (bottom panel) the anticalnexin CT antibody (1:1000 dilution). The relative expression of UGT2B proteins as indicated on the bottom was quantitated on Western blots and normalized to the level of calnexin. The relative quantities of protein are the means of four independent blots.

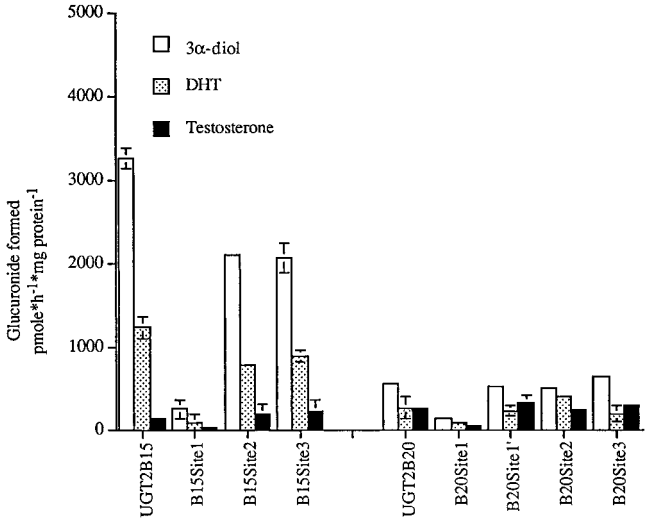

FIGURE 4: Glucuronidation of 3α-diol, testosterone, and DHT by glycosylated and unglycosylated UGT2B15 and UGT2B20 proteins. Activity assays were performed by incubating intact HK293 cells stably expressing UGT2B proteins with radiolabeled substrates. The level of enzyme activity has been normalized to the level of protein expression as determined by Western blot analysis. Values represent the means ± the standard deviation of two experiments each performed in triplicate.

type and mutant proteins on 3α-diol, DHT, and testosterone were determined. Both proteins were active on the three substrates (Figure 4); however, abolishing the first glycosylation site led to decreased activity. Following normalization for variable levels of protein expression, the activities of B15Site1 on 3α-diol, DHT, and testosterone were 13-, 16-, and 4-fold lower than that of the wild type, repectively (Figure 4 and Table 2). Mutation of the glycosylation site in B20Site1 also decreased enzyme activity by 2−5-fold (Figure 4 and Table 2). Mutation of the other N*X*(S/T) sites, which are apparently not glycosylated, had a much lesser or no effect on catalytic activity.

Table 2: Activities of Wild-Type and Glycosylation Mutants of UGT2B15 and UGT2B20 on 3α-Diol, DHT, and Testosterone[a]

	normalized glucuronidation activity [pmol h^{-1} (mg of protein)$^{-1}$]		
protein	3α-diol	DHT	testosterone
UGT2B15	3263 ± 123	1233 ± 129	139 ± 6
B15Site1	241 ± 121	77 ± 10	34 ± 17
B15Site2	2107 ± 20	778 ± 27	181 ± 138
B15Site3	2062 ± 177	891 ± 65	225 ± 132
UGT2B20	551 ± 16	267 ± 129	262 ± 36
B20Site1	145 ± 31	88 ± 13	51 ± 20
B20Site1′	528 ± 27	232 ± 62	321 ± 98
B20Site2	505 ± 6	392 ± 7	244 ± 19
B20Site3	637 ± 15	196 ± 97	287 ± 18

[a] The glucuronidation activities were determined using intact HK293 cells stably expressing the wild-type and mutant proteins. The level of enzyme activity was normalized to the level of protein expression as determined by Western blot analysis. Values represent the means ± the standard deviation of two independent experiments each performed in triplicate.

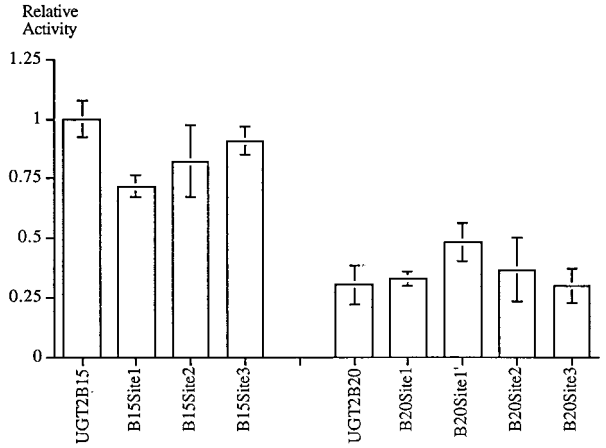

FIGURE 5: Stability analysis of wild-type and N-glycosylation mutants of UGT2B15 and UGT2B20. Each cell line stably expressing the mutant and wild-type UGT2B proteins was treated with 20 μg/mL cycloheximide for 2 h. After treatment, cells were incubated in the presence of cycloheximide and radiolabeled 3α-diol for 6 h, and the level of 3α-diol-G produced was determined. The data represent the means ± the standard deviation of two independent experiments each performed in triplicate.

To determine the influence of glycosylation on the stability of enzyme activities, HK293 cells stably expressing wild-type and mutated proteins were incubated with cycloheximide (20 μg/mL) for 2 h, to arrest de novo protein synthesis, and the level of UGT activity was measured. The B15Site1 had a slight decrease difference in the stability of enzyme activity, based on the formation of 3α-diol-G (Figure 5).

To determine if glycosylation can influence the kinetic properties of UGT2B15 and UGT2B20, the apparent K_m [$K_{m(app)}$] values of 3α-diol and DHT glucuronidation were determined. The values were in the micromolar range, in agreement with previous results (*9*, *26*); however, no

Table 3: Kinetic Analysis of UGT2B15, UGT2B17, and UGT2B20 Mutant Proteins[a]

protein	$K_{m(app)}$ (μM) 3α-diol	DHT
UGT2B20	1.8 ± 0.4	6.0 ± 1.3
UGT2B20 L93I	2.4 ± 0.6	6.3 ± 1.4
UGT2B20 I96R	3.2 ± 0.4	4.7 ± 1.3
UGT2B20 T98I	2.9 ± 0.3	8.7 ± 1.5
UGT2B20 I96R/T98I	2.6 ± 0.4	6.1 ± 1.2
UGT2B15	3.0 ± 0.6	3.0 ± 0.8
UGT2B15 R96I	3.2 ± 0.7	3.8 ± 0.7
UGT2B15 I98T	2.6 ± 0.7	3.6 ± 0.9
UGT2B15 R96I/I98T	3.3 ± 0.5	3.0 ± 0.8
UGT2B17	1.3 ± 0.3	1.3 ± 0.5
UGT2B17 T98I	1.7 ± 0.4	1.0 ± 0.3
B20Site1	2.6 ± 0.7	5.2 ± 0.2
B15Site1	3.8 ± 1.0	2.8 ± 0.2

[a] The apparent K_m values for the conjugation of 3α-diol and DHT were determined using intact HK293 cells stably expressing the exogenous UGT2B proteins. Results represent the means ± the standard deviation of two independent experiments each performed in triplicate.

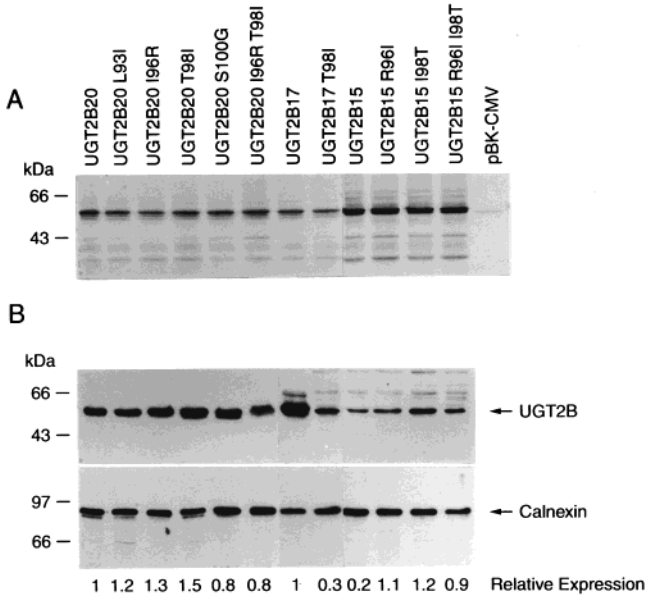

FIGURE 6: (A) In vitro transcription/translation of wild-type and mutant UGT2B cDNA clones and (B) immunoblot analysis of HK293 cells stably expressing the UGT2B proteins. (A) The products of an in vitro transcription/translation reaction of wild-type and mutant UGT2B cDNAs and the pBK-CMV vector were separated by 10% SDS−PAGE. (B) Microsomal proteins (20 μg) from untransfected HK293 cells and HK293 cells stably expressing wild-type and mutated UGT2B15, UGT2B17, and UGT2B20 were separated on a 10% SDS−polyacrylamide gel, transferred onto a nitrocellulose membrane, and probed with (upper panel) the EL-93 anti-UGT2B antisera (1:3000 dilution) or (bottom panel) the anticalnexin CT antibody (1:1000 dilution). The relative expression of UGT2B proteins as indicated on the bottom was quantitated on Western blots and normalized to the level of calnexin. The relative quantities of protein are the means of four independent blots.

difference was observed between the wild-type proteins and B15Site1 and B20Site1 (Table 3).

Involvement of Specific Amino Acids in UGT2B Enzyme Activity. In addition to the role of post-translational modifications on enzyme activity, it was also determined if specific residues in a variable region between the highly homologous UGT2B15, UGT2B17, and UGT2B20 proteins can influence enzymatic properties. Sequence comparison

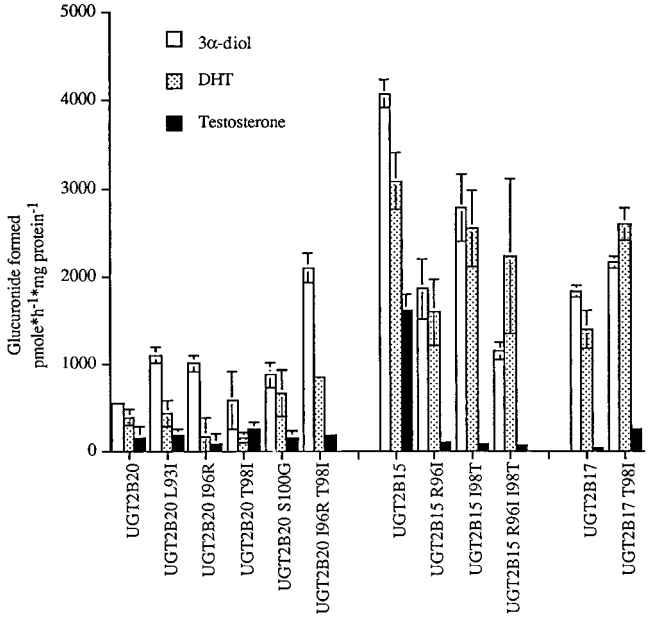

FIGURE 7: Glucuronidation of 3α-diol, testosterone, and DHT by wild-type and mutant UGT2B proteins. Activity assays were performed by incubating intact HK293 cells stably expressing UGT2B proteins with radiolabeled substrates. The level of enzyme activity has been normalized to the level of protein expression as determined by Western blot analysis. Values represent the means ± the standard deviation of two experiments each performed in triplicate.

between the UGT2B proteins revealed a single residue difference at position 96 of UGT2B20, which contains an isoleucine instead of a highly conserved arginine as found in all the other enzymes (Figure 1). Considering the overall level of homology between UGT2B15, UGT2B17, and UGT2B20, which share more than 90% primary structure identity, the region between residues 90 and 100 is strikingly different. (1) The residue at position 93 is different in the three proteins. (2) UGT2B15 contains an isoleucine and a glycine at positions 98 and 100, respectively, whereas UGT2B20 and UGT2B17 have a threonine and a serine at these respective positions. These differences between residues 90 and 100 are within the proposed substrate binding domain of UGT2B proteins, and may influence the stability, substrate specificity, and/or kinetic properties of these enzymes. Thus, residues 93, 96, 98, and 100 of UGT2B15, UGT2B17, and UGT2B20 were changed to assess their involvement in enzyme activity.

Following the introduction of mutations into the cDNA clones, in vitro transcription and translation reactions and stable expression of the cDNAs in HK293 cells produced 51 kDa proteins as expected (Figure 6). To analyze the effect of the mutated residues on substrate specificity and enzyme activity, the activities of mutant UGT2B15, UGT2B17, and UGT2B20 on testosterone, DHT, and 3α-diol were determined, and normalized to the level of protein expressed. All the mutated proteins retained activity for these substrates; however, the level of conjugation for specific substrates was altered in some of the mutants (Figure 7). The double mutation in UGT2B20 I96R/T98I led to a 9.5-fold increase in the level of glucuronidation of 3α-diol which was not observed in the single mutations UGT2B20 I96R and UGT2B20 T98I. Mutation of residue 96 and/or 98 in UGT2B15 decreased the activity on all three substrates,

A

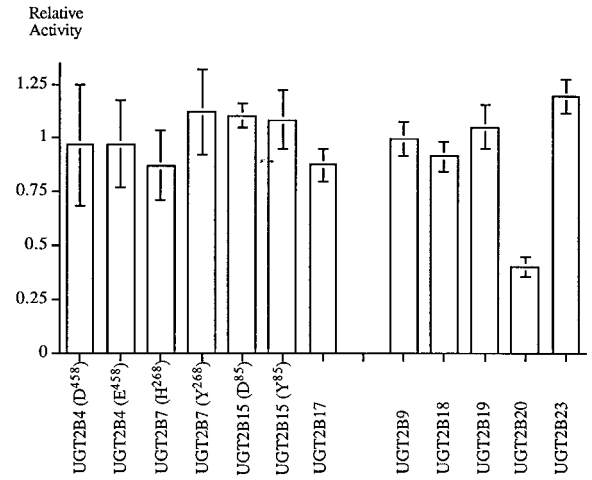

B

Protein	$t_{1/2}$ (hours)
UGT2B4 (D^{458})	10
UGT2B4 (E^{458})	11
UGT2B7 (H^{268})	7
UGT2B7 (Y^{268})	7
UGT2B15 (D^{85})	**> 24**
UGT2B15 (Y^{85})	**> 24**
UGT2B17	3 *
UGT2B9	5
UGT2B18	24
UGT2B19	12
UGT2B20	**0.5**
UGT2B23	18

FIGURE 8: Stability analysis of human and monkey UGT2B proteins. (A) HK293 cell lines stably expressing exogenous proteins were treated with 20 μg/mL cycloheximide for 2 h. After treatment, cells were incubated in the presence of cycloheximide and radiolabeled 3α-diol for 6 h, and the level of 3α-diol-G produced was determined. Results are expressed relative to the untreated control and represent the means ± the standard deviation of two independent experiments each performed in triplicate. (B) To obtain a comparison of the relative stability of enzyme activity between the UGT2B proteins, the stable cell lines were treated with cycloheximide for 1, 2, 4, 6, 8, 10, 12, and 24 h. The time at which 50% of the enzyme activity was lost ($t_{1/2}$) was derived from a plot of relative activity vs time. The values are the mean of two independent experiments each performed in triplicate.

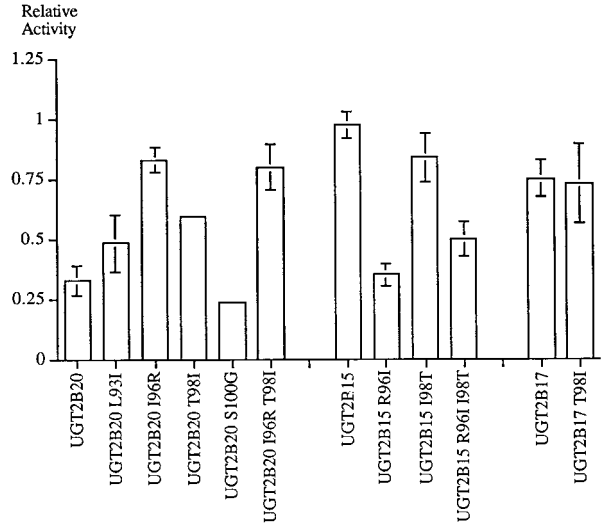

FIGURE 9: Stability analysis of wild-type and mutants of UGT2B15, UGT2B17, and UGT2B20. Each cell line stably expressing the mutant and wild-type UGT2B proteins was treated with 20 μg/mL cycloheximide for 2 h. After treatment, cells were incubated in the presence of cycloheximide and radiolabeled 3α-diol for 6 h, and the level of 3α-diol-G produced was determined. The values are the means ± the standard deviation of two independent experiments each performed in triplicate.

especially on testosterone. In contrast, the UGT2B17 T98I mutant increased glucuronidation activity. None of the mutations had any effect on the specificity on ADT, which can only be conjugated by wild-type and mutant UGT2B17 (data not shown).

Kinetic analysis revealed only slight differences in the apparent K_m values for the conjugation of androgens by the mutant and wild-type proteins. The largest change was a 1.8-fold increase in the $K_{m(app)}$ value for 3α-diol glucuronidation by UGT2B20 I96R, whereas the inverse mutation in UGT2B15 had no effect (Table 3).

Differential Stability of Human and Monkey UGT2B Enzymes. Another parameter that may be modified by specific amino acids is protein stability. Differences in the stability of UGT2B activities have previously been observed by cycloheximide treatment of HK293 cells stably expressing UGT2B15 and UGT2B20. Following cycloheximide treatment for 2 h, UGT2B20 lost more than 50% of its activity, whereas UGT2B15 activity was not affected (*9*, *24*). To assess the stabilities of enzyme activity of the other UGT2B proteins, HK293 cells stably expressing UGT2B4, UGT2B7, UGT2B15, UGT2B17, UGT2B9, UGT2B18, UGT2B19, UGT2B20, and UGT2B23 (and their related polymorphisms) were incubated with cycloheximide (20 μg/mL) for 2 h, and the level of UGT activity was measured by incubation of intact cells with radiolabeled 3α-diol as a substrate (Figure 8A). In agreement with previous results (*24*), the level of UGT2B15 activity was not affected and the level of UGT2B20 was decreased to 38% of the initial activity (*9*). Interestingly, the activities of all the other UGT2B enzymes remained elevated, indicating that only UGT2B20 has a highly labile catalytic activity. To more precisely assess the stability of UGT2B enzyme activity, all the derived cell lines stably expressing the UGT2B proteins were incubated with cycloheximide for 1, 2, 4, 6, 8, 10, 12, and 24 h (Figure 8B). The level of UGT2B20 activity decreased by 50% after approximately 30 min, whereas the activity of UGT2B15 was unchanged after 24 h. The most stable UGT2B enzymes were UGT2B18 and the two variants of UGT2B15, followed by UGT2B23, UGT2B19, the two polymorphisms of UGT2B4 and UGT2B7, and finally UGT2B9, UGT2B17, and UGT2B20. Considering the level of homology between UGT2B9, UGT2B18 (96%), and UGT2B23 (94%) and between UGT2B15 and UGT2B20 (92%), it is apparent that enzyme properties such as stability of activity can vary widely, despite the similarity of protein primary structures (*10*, *29*). Thus, the results suggest that few changes in UGT2B amino acid composition could lead to important differences in enzyme properties. However, it is interesting to note that the natural mutations leading to allelic variants of UGT2B4, UGT2B7, and UGT2B15 do not affect the stability of their activity (Figure 8B), thus indicating that residues at positions 458, 268, and 85 are not involved.

Stability of Wild-Type and Mutant UGT2B Enzyme Activity. To determine the effect of mutations on the stability of enzyme activity, HK293 cells stably expressing wild-type and mutant proteins were incubated with cycloheximide (20 μg/mL) for 2 h, and the level of UGT activity was measured

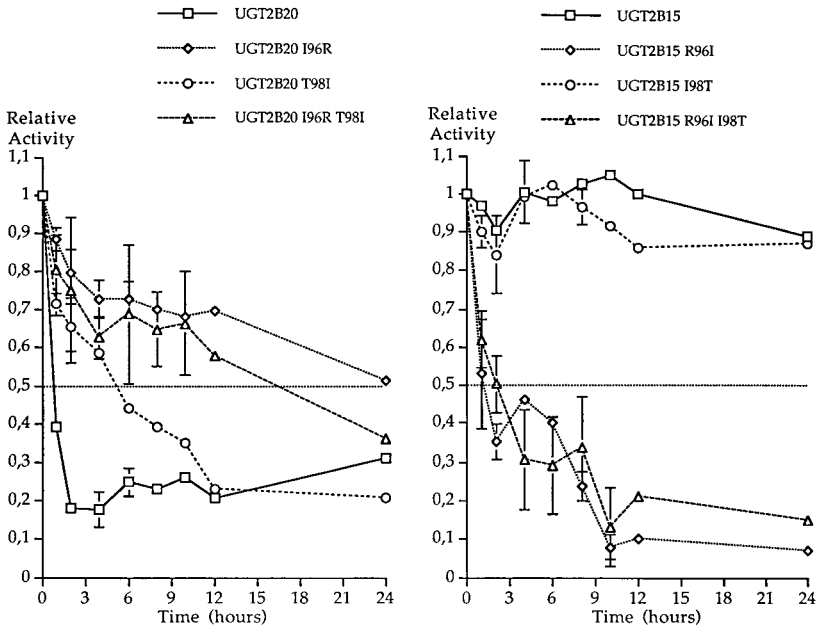

FIGURE 10: Stability analysis of human UGT2B15, monkey UGT2B20, their related position 96 or 98 mutants, and double-mutant (positions 96 and 98) proteins. UGT2B stable cell lines were treated with 20 μg/mL cycloheximide for 1, 2, 4, 6, 8, 10, 12, and 24 h. After treatment, cells were incubated in the presence of cycloheximide and radiolabeled 3α-diol. The dashed line indicates the 50% level of relative activity. The results at each time point are from two independent experiments each performed in triplicate ± the standard deviation.

by incubation of intact cells with radiolabeled 3α-diol as the substrate. The results demonstrate that the UGT2B20 I96R, UGT2B20 T98I, and UGT2B20 I96R/T98I mutants have higher activity than the wild-type enzyme (Figure 9). Interestingly, the corresponding mutations in UGT2B15 (UGT2B15 R96I and UGT2B15 R96I/I98T) have the opposite effect, where activity was decreased after arresting protein synthesis for 2 h (Figure 9). To further investigate the role of positions 96 and 98 in enzyme stability, HK293 cells stably expressing UGT2B20, UGT2B20 I96R, UGT2B20 T98I, UGT2B20 I96R/T98I, UGT2B15, UGT2B15 R96I, UGT2B15 I98T, or UGT2B15 R96I/I98T were incubated in the presence of cycloheximide for 1, 2, 4, 6, 8, 10, 12, and 24 h (Figure 10). The change of the isoleucine found at position 96 of UGT2B20 to an arginine as found in UGT2B15 led to a more stable UGT2B20 I96R protein ($t_{1/2}$ = 24 h), while the inverse mutation in UGT2B15 R96I yielded a protein with a shorter half-life ($t_{1/2}$ = 1 h) similar to wild-type UGT2B20. The mutation of residue 98 did not affect the stability of UGT2B15 activity, while the half-life of UGT2B20 T98I activity was higher than that of the wild-type enzyme (Figure 10). The double mutants, UGT2B20 I96R/T98I and UGT2B15 R96I/I98T, yielded the same results as proteins with a single mutation at position 96. These results suggest that the residue at position 96 plays an important role in the stability of human and monkey UGT2B enzyme activity, while position 98 is less involved (Figure 10). The mutation in UGT2B17 T98I also did not alter the stability of enzyme activity (Figure 9).

Correlation between Residue 96, Protein Secondary Structure, and Enzyme Stability. Six different algorithms of protein secondary structure prediction were utilized to analyze the potential effect(s) that the mutation at residue 96 may have in UGT2B15 and UGT2B20 (Figure 11). Each algorithm predicted an α-helix between residues 84 and 100 in both proteins; however, the length and position of the α-helix are variable depending on the program that is used (Figure 11). In all cases, the α-helix is longer in UGT2B15 than in UGT2B20, and exchange of the Ile96 in UGT2B20 for the Arg of UGT2B15 led to a lengthening of the α-helix (Figure 11). In contrast, the reciprocal mutation in UGT2B15 led to a shorter α-helix. In addition, on the basis of the algorithms of Levin (*33*) and Frishman and Argos (*35*), the α-helix between amino acids 84 and 100 in UGT2B20 is the shortest of all the known mammalian UGT2B proteins (Figure 12). The other mutations in UGT2B20, UGT2B15, and UGT2B17 do not affect this α-helix. Thus, these results taken together suggest that the isoleucine at position 96 of UGT2B20 reduces the length of an α-helix, which correlates with a decreased stability of enzyme activity.

DISCUSSION

Recent results have highlighted the potential role of UDP-glucuronosyltransferase enzymes in the metabolism of steroid hormones. The demonstration of UGT1A and UGT2B enzyme activities on specific steroids and the expression of UGT transcripts and proteins in extrahepatic steroid target tissues indicate that glucuronidation is potentially a pathway by which steroids can be metabolized, transported from the tissue into the circulation, and subsequently eliminated from the body via the bile and urine. Due to the potential physiological role of these enzymes in steroid metabolism, it is reasonable to expect some degree of regulation at the level of UGT expression and activity, which would be required as these enzymes respond to physiological needs. Previous results have demonstrated that the expression of UGT2B genes can be differentially regulated, where the steady state levels of human UGT2B15 and UGT2B17 transcripts respond differently when LNCaP cells are treated with EGF, DHT (*39*), FGF (*40*), and interleukin-1α (*41*). It is interesting that expression of the more labile UGT2B17 protein is regulated by EGF and DHT, whereas expression of the highly stable UGT2B15 protein does not respond to

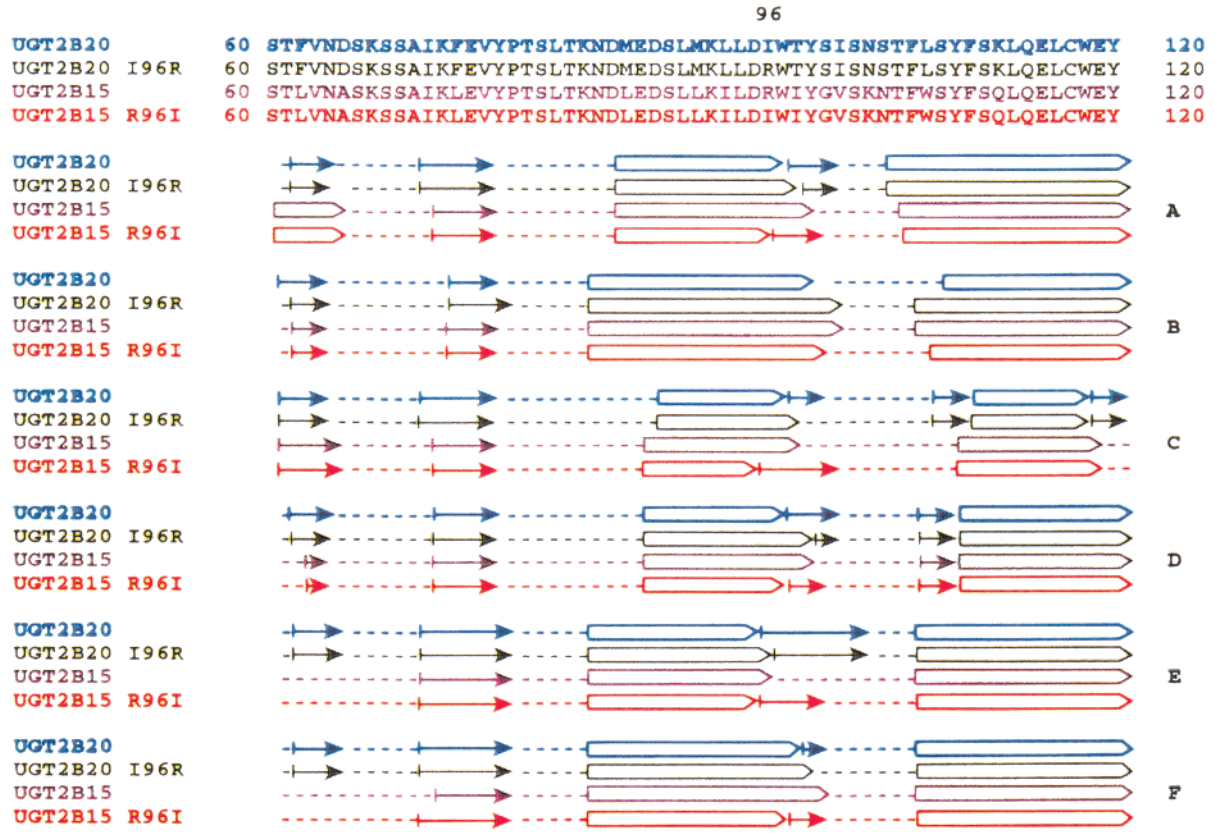

FIGURE 11: Protein secondary structure prediction for UGT2B20 (blue), UGT2B20 R96I (black), UGT2B15 (pink), and UGT2B15 I96R (red). The protein secondary structure predictions for the region between residues 60 and 120 were obtained using six different programs: (A) J. Levin, (B) B. Rost and C. Sander, (C) D. Frishman and P. Argos, (D) D. G. Kneller et al., (E) T. Ti and E. Lander, and (F) J. U. Bowie. A large open arrow represents a potential α-helix; a thin arrow represents a potential *β*-strand, and dashed lines represent turns.

these effectors. Although these two enzymes have overlapping substrate specificities, these results are consistent with expression of the more labile protein being regulated to respond to changing physiological requirements. Recent studies have demonstrated the ability of the *UGT2B17* gene promoter region to respond to physiological effectors (*39*), and comparison between the *UGT2B15* and *UGT2B17* gene 5′-flanking DNA sequences has identified differences in potential cis-acting elements that may explain the differential regulation of these two highly related genes (*42*). However, in addition to transcriptional regulation, analysis of the UGT2B protein primary structures reveals putative N-linked glycosylation sites, which may potentially influence enzyme functions.

Most of the mammalian UGT2B proteins characterized to date have two or three potential N-linked glycosylation sites with the sequence N*X*(S/T). However, the notable exceptions are UGT2B4 and UGT2B20, which have one and four sites, respectively. Although it has been shown that some UGT proteins are N-glycosylated, the role of this post-translational modification is not well-understood in these enzymes. The treatment of rat UGT2B1, UGT2B2, and UGT2B6 with glycopeptidases did not have any effects on catalytic activities (*43*); however, Mackenzie (*11*) reported that deglycosylation of rat UGT2B1 decreased the rate of enzyme activity, without any effect on protein stability and substrate specificity. However, the number and identities of the relevant glycosylation sites were not determined in these studies. Using endoglycosidase H digestion and SDS−PAGE, the study presented here demonstrates that human and monkey UGT2B proteins are differentially glycosylated. There was no evidence of glycosylation in human UGT2B4 and monkey UGT2B18 and UGT2B23, whereas protein glycosylation of human UGT2B7, UGT2B15, and UGT2B17 and monkey UGT2B20 was apparent. However, the results for monkey UGT2B9 and UGT2B19 are inconclusive. The proteins UGT2B7, UGT2B9, UGT2B18, UGT2B19, and UGT2B23 share very similar glycosylation sites, but only UGT2B7 is clearly glycosylated. This apparent differential glycosylation of human and monkey UGT2B proteins was also previously noted with rat proteins, where UGT2B1 and UGT2B2 are substrates for endoglycosidase H, while UGT2B6 is not glycosylated (*43*). Thus, despite the high level of homology between these proteins, it is apparent that the extent of UGT2B protein glycosylation cannot be predicted on the basis of the presence or location of the consensus N-linked glycosylation sequences N*X*(S/T).

Initial characterization of UGT2B20 demonstrated a level of primary structure identity of 92% with UGT2B15, which is higher than with any other UGT2B protein (simian or human) characterized to date (*9*). Moreover, UGT2B20 and UGT2B15 have similar substrate specificities and kinetic properties for androgen glucuronidation (*9*, *26*); however, one striking difference is the presence of an additional putative N-linked glycosylation site at residue 103 in UGT2B20 (Figure 1). Site-directed mutagenesis of the individual sites in UGT2B15 and UGT2B20 demonstrates a similar pattern of glycosylation in both proteins, where only the first site from the amino terminus at position 65 is glycosylated, and the additional site in UGT2B20 is not used.

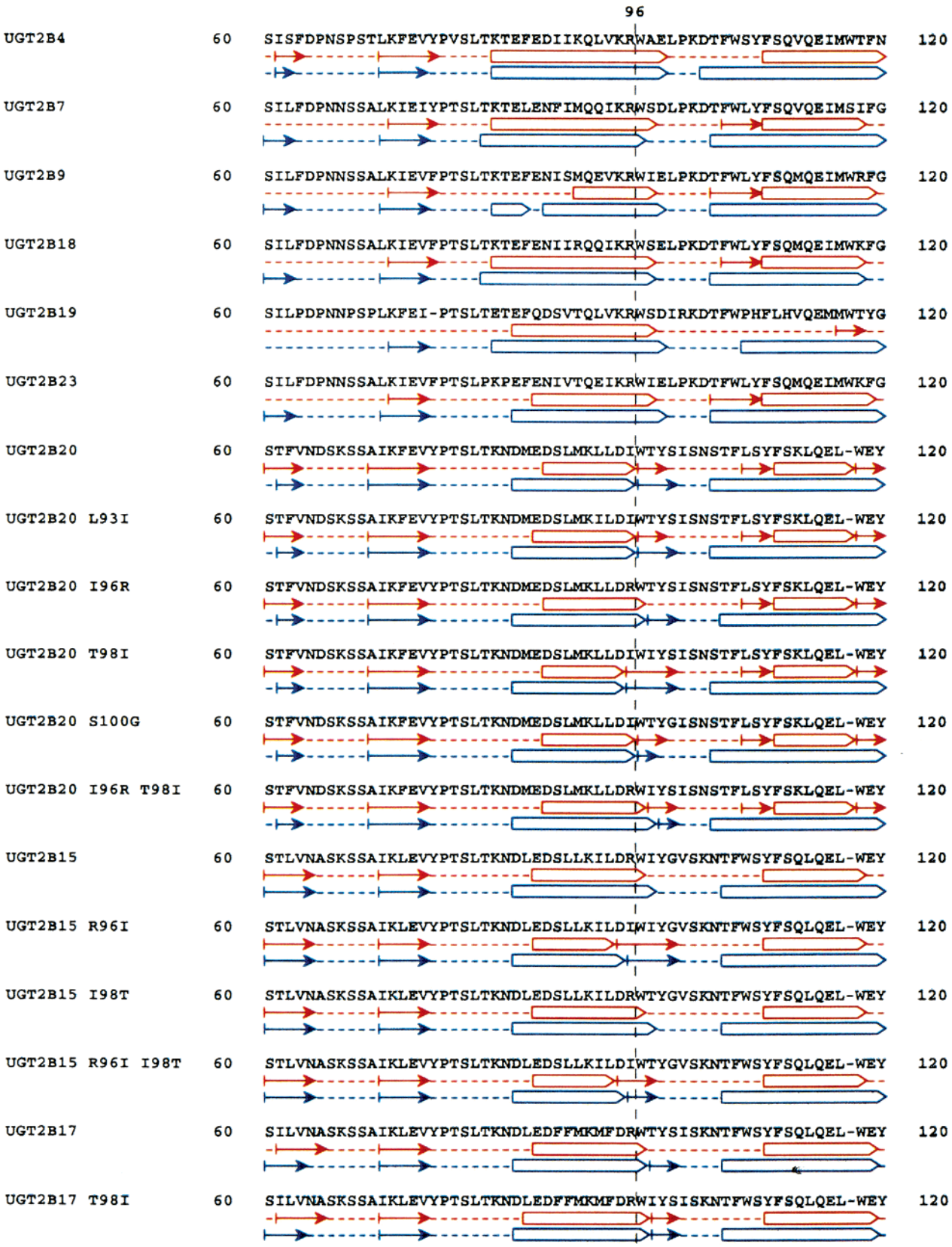

FIGURE 12: Protein secondary structure predictions for the mutant and wild-type UGT2B proteins. The secondary structure predictions were determined using the programs of J. Levin (red) and D. Frishman and P. Argos (blue).

Abolishing the site of glycosylation in both proteins led to reduced glucuronidation activity without any effect on substrate specificity and apparent K_m values. To verify that the reduced enzyme activities were due to abolition of glycosylation and not due to the changes in primary structures, the effects of treatment with tunicamycin D on wild-type UGT2B15 and UGT2B20 and with endoglycosidase H on wild-type UGT2B15 and UGT2B19 on microsome extracts were analyzed. The results demonstrated that treated UGT2B15 and UGT2B20 had dramatically reduced activity,

while endoglycosidase H treatment did not affect the glucuronidation activity of the unglycosylated UGT2B19 enzyme (data not shown). Studies on other proteins have revealed the importance of glycosylation on enzyme function. The removal of N-linked oligosaccharide chains on human gastric lipase or human and rat β-glucuronidase led to reduced protein activity, whereas a decreased level of receptor binding was observed with deglycosylated rat placental lactogen (*5*, *6*, *44*). In other cases, glycosylation can affect substrate affinity without changing enzyme velocity, as shown with human glucose transporter 1 (*45*). Genetic polymorphisms affecting protein glycosylation have also been correlated with diseases such as with the luteinizing hormone β-subunit gene, where an additional N-linked glycosylation site led to infertility (*46*), and with the sex hormone-binding globulin, where an additional N-glycosylation site is highly correlated with estrogen-dependent breast cancer (*47*). Although protein glycosylation has also been shown to affect enzyme stability (*48*), the removal of the glycosylated site on UGT2B20 had no effect on the stability of this labile enzyme.

The glycosylation of UGT2B proteins is a potential mechanism whereby the rates of enzyme activity can be regulated. In addition to the results in this study, which indicate differential glycosylation of different UGT2B proteins, previous results suggest tissue specific glycosylation of UGT2B proteins. Western blot analysis of microsome preparations from different tissues reveals additional immunoreactive UGT2B proteins with higher apparent molecular masses, which is indicative of glycosylation, in some tissues such as the kidney but not in other tissues such as the prostate (*49*). Since these tissues express many UGT2B transcripts in common, including UGT2B20, these results raise the possibility that UGT2B proteins are glycosylated in a tissue specific manner. Although it is not known how UGT2B protein glycosylation is regulated, there is evidence that glycosylation can be regulated by effectors such as the fibroblast platelet-derived growth factor, which stimulates N-linked glycosylation of the insulin growth factor receptor and increases its rate of translocation to the cell surface (*50*). In addition, prolactin has been reported to induce the expression of enzymes involved in terminal glycosylation (*7*), and interleukin-2 can induce a 10-fold increase in N-glycosylation activity during the late phase of T-cell activation (*51*). Although the UGT2B proteins have been demonstrated to be glycosylated and may play a role in influencing enzyme activity, it remains to be determined if this post-translational modification is regulated in this family of enzymes.

The comparison of primary structures between the highly homologous UGT2B proteins reveals regions and residues, which may potentially be involved in the differences of enzymatic properties. In general, the amino regions of the proteins are more variable than the carboxyl regions, which is consistent with the hypothesis of the amino region containing the substrate specific aglycone binding domain and the carboxyl region containing the UDP-glucuronic acid binding domain (*16*). Between the highly homologous UGT2B15 and UGT2B20 proteins, 30 of the 41 amino acid differences (*9*) are found between residues 1 and 290, which includes the region from position 60 to 120 proposed to be important for substrate binding (*52*). A region of high variability is found between residues 90 and 100. The importance of this region is shown by the mutants UGT2B20 I96R/T98I, UGT2B15 R96I, UGT2B15 I98T, and UGT2B15 R96I/I98T, which led to proteins with altered enzyme activity. In addition, a previous study (*22*) showed that a double mutation in UGT2B17 (M93I/F94L) abolished enzyme activity.

Alignment of all the UGT2B protein primary structures revealed a striking difference at position 96 in UGT2B20, which contains an isoleucine instead of an arginine residue as found in all the other mammalian UGT2B proteins characterized to date. Changing the isoleucine residue in UGT2B20 to an arginine altered the level of activity on 3α-diol, and increased the stability of enzyme activity. To determine if the increased stability is related to changes in protein structure, secondary structure prediction programs revealed the presence of an α-helix in the region between residues 84 and 100. Although the length of the α-helix is slightly different depending on the program that is used, the helix in UGT2B20 is consistently the shortest when compared to those of all the other mammalian UGT2B proteins. The amino acid change in UGT2B20 I96R led to a longer predicted α-helix, which suggests that the length of the helix between residues 84 and 100 influences the stability of enzyme activity. In agreement with this hypothesis, changing the residue at position 96 from an arginine to an isoleucine in UGT2B15 R96I led to a shorter predicted α-helix and a decrease in enzyme stability. From these results, it is apparent that the length of the α-helix between residues 84 and 100 plays an important role in the stability of catalytic activity in UGT2B enzymes. However, it is also apparent that other residues are involved in conferring enzyme stability, since although the activity of UGT2B20 I96R is more stable than wild-type UGT2B20, it is still more labile than UGT2B15. Although the mechanism involved in the stabilization of UGT2B20 I96R is unknown, results suggest that the high labilities of UGT2B20 and UGT2B17 are conferred differently. The decreased activity of UGT2B20 in cells treated with cycloheximide is not associated with amounts of protein, which remained unchanged throughout all treatments as observed in Western blots (*9*). However, similar experiments with the labile UGT2B17 protein show a correlation between decreased enzyme activity and protein levels (D. Turgeon, personal communication). A possible function of these highly labile UGT2B proteins is that induced glucuronidation of specific aglycons may be required for a narrow time frame in a specific cell type, in response to physiological needs.

Although the mammalian UGT2B enzymes are highly conserved, it has been shown that their expressions are differentially regulated by physiological effectors, they have different stabilities, and they possess overlapping but distinct patterns of substrate specificity. Thus, to understand the physiological role of the individual UGT2B proteins, it is important to decipher the mechanisms responsable for the differences observed between these enzymes. The results in this study indicate that although all mammalian UGT2B enzymes contain consensus N-linked glycosylation sites, they are differentially glycosylated, and this modification can influence the velocity of enzyme activity. It was also shown that the length of a putative α-helix between residues 84 and 100 is associated with the stability of the catalytic activity of UGT2B enzymes. It is apparent that other differences in

the primary structures of UGT2B proteins are also involved in conferring differences of enzyme properties, which will most probably be important in the physiological functions of these enzymes.

ACKNOWLEDGMENT

We thank Dr. Pei Min Rong and Pierre-Michel Simard for their excellent technical assistance in Western blot analysis and DNA sequencing.

REFERENCES

1. Dutton, G. J. (1980) in *Glucuronidation of drugs and other compounds*, CRC Press, Boca Raton, FL.
2. Mackenzie, P. I., Owens, I. S., Burchell, B., Bock, K. W., Bairoch, A., Bélanger, A., Fournel-Gigleux, S., Green, M., Hum, D. W., Iyanagi, T., Lancet, D., Louisot, P., Magdalou, J., Chowdhury, J. R., Ritter, J. K., Schachter, H., Tephly, T. R., Tipton, K. F., and Nebert, D. W. (1997) *Pharmacogenetics 7*, 255−269.
3. Hum, D. W., Bélanger, A., Lévesque, É., Barbier, O., Beaulieu, M., Albert, C., Vallée, M., Guillemette, C., Tchernoff, A., Turgeon, D., and Dubois, S. (1999) *J. Steroid Biochem. Mol. Biol. 69*, 413−423.
4. Rosenfeld, M. G., Kreibich, G., Popov, D., Kato, K., and Sabatini, D. D. (1982) *J. Cell Biol. 93*, 135−143.
5. Wicker-Planquart, C., Canaan, S., Riviere, M., and Dupuis, L. (1999) *Eur. J. Biochem. 262*, 644−651.
6. Shipley, J. M., Grubb, J. H., and Sly, W. S. (1993) *J. Biol. Chem. 268*, 12193−12198.
7. Bolander, F. F., Jr. (1999) *Mol. Cell. Endocrinol. 149*, 85−92.
8. Battaglia, E., Nowell, S., Drake, R. R., Magdalou, J., Fournel-Gigleux, S., Senay, C., and Radominska, A. (1997) *Drug Metab. Dispos. 25*, 406−411.
9. Barbier, O., Bélanger, A., and Hum, D. W. (1999) *Biochem. J. 337*, 567−574.
10. Barbier, O., Lévesque, E., Bélanger, A., and Hum, D. W. (1999) *Endocrinology 140*, 5538−5548.
11. Mackenzie, P. I. (1990) *Biochem. Biophys. Res. Commun. 166*, 1293−1299.
12. Lidholt, K., Weinke, J. L., Kiser, C. S., Lugemwa, F. N., Bame, K. J., Cheifetz, S., Massague, J., Lindahl, U., and Esko, J. D. (1992) *Proc. Natl. Acad. Sci. U.S.A. 89*, 2267−2271.
13. Meissner, J. D., Naumann, A., Mueller, W. H., and Scheibe, R. J. (1999) *Biochem. J. 338*, 561−568.
14. Brierley, C. H., Senafi, S. B., Clarke, D., Hsu, M. H., Johnson, E. F., and Burchell, B. (1996) *Adv. Enzyme Regul. 36*, 85−97.
15. Tephly, T. R. (1990) *Chem. Res. Toxicol. 3*, 509−516.
16. Meech, R., and Mackenzie, P. I. (1997) *Clin. Exp. Pharmacol. Physiol. 24*, 907−915.
17. Mackenzie, P. I. (1990) *J. Biol. Chem. 265*, 3432−3435.
18. Ritter, J. K., Chen, F., Sheen, Y. Y., Lubet, R. A., and Owens, I. S. (1992) *Biochemistry 31*, 3409−3414.
19. Senay, C., Ouzzine, M., Battaglia, E., Pless, D., Cano, V., Burchell, B., Radominska, A., Magdalou, J., and Fournel-Gigleux, S. (1997) *Mol. Pharmacol. 51*, 406−413.
20. Meech, R., Yogalingam, G., and Mackenzie, P. I. (1996) *DNA Cell Biol. 15*, 489−494.
21. Li, Q., Lou, X., Peyronneau, M. A., Straub, P. O., and Tukey, R. H. (1997) *J. Biol. Chem. 272*, 3272−3279.
22. Dubois, S., Beaulieu, M., Lévesque, É., Hum, D. W., and Bélanger, A. (1999) *J. Mol. Biol. 289*, 29−39.
23. Chen, F., Ritter, J. K., Wang, M. G., Mcbride, O. W., Lubet, R. A., and Owens, I. S. (1993) *Biochemistry 32*, 10648−10657.
24. Guillemette, C., Lévesque, É., Beaulieu, M., Turgeon, D., Hum, W. D., and Bélanger, A. (1997) *Endocrinology 138*, 2998−3005.
25. Lévesque, É., Beaulieu, M., Hum, D. W., and Bélanger, A. (1999) *Pharmacogenetics 9*, 207−216.
26. Lévesque, É., Beaulieu, M., Green, M. D., Tephly, T. R., Bélanger, A., and Hum, D. W. (1997) *Pharmacogenetics. 7*, 317−325.
27. Beaulieu, M., Lévesque, É., Hum, D. W., and Bélanger, A. (1996) *J. Biol. Chem. 271*, 22855−22862.
28. Coffman, B. L., King, C. D., Rios, G. R., and Tephly, T. R. (1998) *Drug Metab. Dispos. 26*, 73−77.
29. Beaulieu, M., Lévesque, É., Barbier, O., Turgeon, D., Bélanger, G., Hum, D. W., and Bélanger, A. (1998) *J. Mol. Biol. 275*, 785−794.
30. Bélanger, G., Beaulieu, M., Lévesque, E., Hum, D. W., and Bélanger, A. (1997) *DNA Cell Biol. 16*, 1195−1205.
31. Bélanger, G., Barbier, O., Hum, D. W., and Bélanger, A. (1999) *Eur. J. Biochem. 260*, 701−708.
32. Guillemette, C., Hum, D. W., and Bélanger, A. (1995) *J. Steroid Biochem. Mol. Biol. 55*, 355−362.
33. Levin, J. (1997) *Protein Eng. 7*, 771−776.
34. Rost, B., and Sander, C. (1994) *Proteins 19*, 55−72.
35. Frishman, D., and Argos, P. (1996) *Protein Eng. 9*, 133−142.
36. Kneller, D. G., Cohen, F. E., and Langridge, R. (1990) *J. Mol. Biol. 214*, 171−182.
37. Yi, T. M., and Lander, E. S. (1993) *J. Mol. Biol. 232*, 1117−1129.
38. Bowie, J. U., Luthy, R., and Eisenberg, D. (1991) *Science 253*, 164−170.
39. Beaulieu, M., Lévesque, E., Tchernof, A., Beatty, B. G., Bélanger, A., and Hum, D. W. (1997) *DNA Cell Biol. 16*, 1143−1154.
40. Lévesque, É., Beaulieu, M., Guillemette, C., Hum, D. W., and Bélanger, A. (1998) *J. Steroid Biochem. Mol. Biol. 64*, 43−48.
41. Lévesque, É., Beaulieu, M., Guillemette, C., Hum, D. W., and Bélanger, A. (1998) *Endocrinology 139*, 2375−2381.
42. Turgeon, D., Carrier, J. S., Lévesque, E., Beatty, B. G., Hum, D. W., and Bélanger, A. (2000) *J. Mol. Biol. 285*, 486−504.
43. Green, M. D., and Tephly, T. R. (1989) *Arch. Biochem. Biophys. 273*, 72−78.
44. Hattori, N., Nukada, T., Oda, M., Tanaka, S., Ogawa, T., and Shiota, K. (1998) *Endocr. J. 45*, 659−674.
45. Ahmed, N., and Berridge, M. V. (1999) *Leuk. Res. 23*, 395−401.
46. Huhtaniemi, I., Jiang, M., Nilsson, C., and Pettersson, K. (1999) *Mol. Cell. Endocrinol. 151*, 89−94.
47. Becchis, M., Frairia, R., Ferrera, P., Fazzari, A., Ondei, S., Alfarano, A., Coluccia, C., Biglia, N., Sismondi, P., and Fortunati, N. (1999) *Breast Cancer Res. Treat. 54*, 101−107.
48. Dennis, J. W., Granovsky, M., and Warren, C. E. (1999) *Bioassays 21*, 412−421.
49. Albert, C., Barbier, O., Vallée, M., Beaudry, G., Bélanger, A., and Hum, D. W. (2000) *Endocrinology 141*, 2472−2480.
50. Carlberg, M., and Larson, O. (1996) *Exp. Cell Res. 223*, 142−148.
51. Kumar, V., Heinemann, F. S., and Ozols, J. (1998) *Biochem. Biophys. Res. Commun. 247*, 524−529.
52. Tephly, T. R., and Burchell, B. (1990) *Trends Pharmacol. Sci. 11*, 276−279.

BI000779P